Inhibition of Staphyloxanthin Virulence Factor Biosynthesis in *Staphylococcus aureus*: In Vitro, in Vivo, and Crystallographic Results†

Yongcheng Song,‡ Chia-I Liu,§,¶,⊥ Fu-Yang Lin,◆ Joo Hwan No,◆ Mary Hensler,# Yi-Liang Liu,◆ Wen-Yih Jeng,§,¶,⊥ Jennifer Low,|| George Y. Liu,|| Victor Nizet,# Andrew H.-J. Wang,§,¶,⊥ and Eric Oldfield*,‡,◆

Department of Chemistry and Center for Biophysics and Computational Biology, University of Illinois at Urbana−Champaign, 600 S. Mathews Avenue, Urbana, Illinois 61801, Institute of Biological Chemistry, Academia Sinica, Nankang, Taipei 11529, Taiwan, National Core Facility of High-Throughput Protein Crystallography, Academia Sinica, Nankang, Taipei 11529, Taiwan, Institute of Biochemical Sciences, College of Life Science, National Taiwan University, Taipei 10098, Taiwan, Department of Pediatrics and Skaggs School of Pharmacy and Pharmaceutical Sciences, University of California, San Diego, 9500 Gilman Drive, La Jolla, CA, and Division of Pediatric Infectious Diseases and Immunobiology Research Institute, Cedars-Sinai Medical Center, Los Angeles, California 90048

Received February 11, 2009

The gold color of *Staphylococcus aureus* is derived from the carotenoid staphyloxanthin, a virulence factor for the organism. Here, we report the synthesis and activity of a broad variety of staphyloxanthin biosynthesis inhibitors that inhibit the first committed step in its biosynthesis, condensation of two farnesyl diphosphate (FPP) molecules to dehydrosqualene, catalyzed by the enzyme dehydrosqualene synthase (CrtM). The most active compounds are phosphonoacetamides that have low nanomolar K_i values for CrtM inhibition and are active in whole bacterial cells and in mice, where they inhibit *S. aureus* disease progression. We also report the X-ray crystallographic structure of the most active compound, *N*-3-(3-phenoxyphenyl)propylphosphonoacetamide ($IC_{50} = 8$ nM, in cells), bound to CrtM. The structure exhibits a complex network of hydrogen bonds between the polar headgroup and the protein, while the 3-phenoxyphenyl side chain is located in a hydrophobic pocket previously reported to bind farnesyl thiodiphosphate (FsPP), as well as biphenyl phosphonosulfonate inhibitors. Given the good enzymatic, whole cell, and in vivo pharmacologic activities, these results should help guide the further development of novel antivirulence factor-based therapies for *S. aureus* infections.

Introduction

Infections caused by *Staphylococcus aureus* are a growing cause of concern[1,2] because of the widespread development of antibiotic resistance and the shortfall in the introduction of new types of anti-infective agents. An alternative strategy that is now gaining interest is targeting of bacterial virulence factors,[3−5] molecules that are essential for bacterial growth and/or invasiveness in vivo. Since these factors are by definition not essential for survival in vitro, screening for virulence factor inhibitors can be challenging. However, at least in the case of *S. aureus*,[6,7] one important virulence factor is a brightly colored carotenoid pigment, staphyloxanthin (STX[a]), whose biosynthesis can be readily monitored spectrophotometrically. The carotenoid is produced by the condensation of the C_{15} isoprenoid farnesyl diphosphate (FPP) to form presqualene diphosphate and then dehydrosqualene, followed by a series of oxidations and glycosylations, in a series of reactions catalyzed by the enzymes CrtM, N, O, P,...,[8] and inhibition of these enzymes (e.g., CrtN by diphenylamine) has been known for many years to result in colorless bacteria.[9,10] In later work,[6] it was shown that loss of the STX pigment made *S. aureus* susceptible to killing by reactive oxygen species (ROS, such as H_2O_2, ClO^-, OH) produced by neutrophils, blocking infectivity. Consequently, inhibition of staphyloxanthin biosynthesis is a potential novel target of anti-infective therapy against pigmented *S. aureus* strains.[11−13]

The first committed step in staphyloxanthin biosynthesis (Figure 1) involves the condensation of two FPP molecules to form dehydrosqualene. This reaction is thought to occur via a presqualene diphosphate intermediate and is very similar (or identical) to that catalyzed by squalene synthase (SQS) in plants, animals, and some protozoa, where the squalene so produced is then converted into sterols such as cholesterol, ergosterol, and the plant sterols. It was thus of interest to see if any of the many known SQS inhibitors previously developed as cholesterol lowering drug leads might also have activity in blocking staphyloxanthin biosynthesis and hence *S. aureus* virulence. We recently reported that one class of inhibitor, phosphonosulfonates, did exhibit such activity.[14] The phosphonosulfonates (and related bisphosphonates) were developed earlier by Magnin et al.[15,16] using FPP as a "template". The bisphosphonate analogues of FPP tended to bind to bone and also caused elevation of liver enzyme function, and the farnesyl side chain was metabolically reactive. However, the phosphonosulfonates did not have these drawbacks, and replacement of the farnesyl side chain by a diphenyl ether removed the metabolic instability. Using **1**, we found good CrtM inhibition restored ROS (H_2O_2, neutrophil) sensitivity and, importantly, observed a major decrease in bacterial burden following *S. aureus* challenge in mice.[14] There are, however, many other conceivable backbones (as well as side chains) that might also have good or even better

† Crystal structure coordinates have been deposited in the Protein Data Bank and will be released upon publication (2ZY1).

* To whom correspondence should be addressed. Phone: 217-333-3374. Fax: 217-244-0997. E-mail: eo@chad.scs.uiuc.edu.

‡ Department of Chemistry, University of Illinois at Urbana−Champaign.

§ Institute of Biological Chemistry.

¶ National Core Facility of High-Throughput Protein Crystallography.

⊥ National Taiwan University.

◆ Center for Biophysics and Computational Biology, University of Illinois at Urbana−Champaign.

University of California, San Diego.

|| Cedars-Sinai Medical Center.

[a] Abbreviations: CrtM, dehydrosqualene synthase; FPP, farnesyl diphosphate; QSAR, quantitative structure−activity relationship; SQS, squalene synthase; STX, staphyloxanthin.

10.1021/jm9001764 CCC: $40.75

activity. To explore some of these possibilities, we were particularly interested to see if it might be possible to reduce backbone charge/acidity/polarity while still retaining CrtM activity, since this might improve inhibitor uptake into bacterial and host cells, as well as further reducing bone affinity. The possibility that less polar analogues might still have good activity is supported by the observation that, unlike bisphosphonate inhibitors of farnesyl diphosphate synthase (FPPS), our published CrtM results indicated that Mg^{2+} binding (which usually involves binding to two anionic groups) is not essential for potent phosphonosulfonate inhibition of CrtM.[14] For example, while **1** binds to CrtM with two Mg^{2+} (PDB file 2ZCQ), **2** binds with only one Mg^{2+} (PDB file 2ZCR), and **3** has no Mg^{2+} at all in its X-ray crystallographic structure (PDB file 2ZCS). So, unlike the situation found with FPPS, it seemed likely that a broad range of backbone structures having fewer anionic groups might be developed, since the number of metal ions involved in binding to CrtM is quite variable.

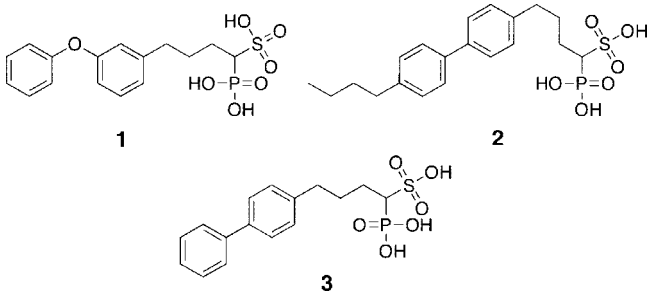

In this work, we describe the synthesis of, and inhibition by, 18 compounds encompassing the 11 basic structural motifs (**a**−**k**) shown in Figure 2 in which Ar is an aromatic fragment. Since some compounds were prepared as salts while others were free acids, these motifs are shown for simplicity in their protonated or free acid forms, a point we discuss later in the text. These motifs were designed on the basis of the following ideas: In **a**, we reduced the (potentially) −3 formal side chain charge found in the phosphonosulfonates ($-PO_3H_2/-PO_3^{2-}$, $-SO_3H/-SO_3^-$) to −2 but added a H-bond donor/acceptor amide site, a feature suggested at least in part because of synthetic accessibility. In all cases, the number of methylene groups n in the "spacer" (Figure 2) was in the range $n = 2-4$, typically $n = 3$, and the Ar groups were diphenyl ethers or biphenyls. In **b** and **c** we reduced the side chain formal charge to −1, but of course the sulfonic and carboxylic acids are expected to have very different pK_a values. In **d** and **e** we investigated whether methyl substitutions might affect activity, while in **f** we investigated the effect of modifying H-bond donor ability. In **g**−**i** we further investigated the role of H-bonding, while in **j**, we attempted to design a novel motif that might facilitate metal binding. Finally, compound **k** (a phosphinomethylphosphonate) was included as a nonhydrolyzable diphosphate analogue (replacing two −O− linkages with two $-CH_2-$). We also report the X-ray crystallographic structure of one of the most potent CrtM/STX biosynthesis inhibitors (containing motif **a**) bound to CrtM, which gives interesting new insights into how this compound binds to its CrtM target.

Results and Discussion

We synthesized a total of 18 compounds (**4**−**21**) based on the 11 motifs shown in Figure 2, and the structures of these compounds are shown in Table 1, rank-ordered in terms of decreasing activity in CrtM inhibition. The K_i values were determined by using a coupled diphosphate/phosphate release assay,[17] as described in the Experimental Section, and are also reported in Table 1. As can be seen in Table 1, the most potent inhibitors (**4**−**6**) were all diphenyl ether phosphonoacetamides (motif **a**, Figure 2) containing a $(CH_2)_3$ spacer between the aromatic and amide moiety and had K_i values in the range 30−70 nM, slightly greater than the 20 nM found for the lead phosphonsulfonate **1** in the same assay. The activities of these three compounds in the inhibition of STX biosynthesis in *S. aureus* are also shown in Table 1, from which we see that **5** is the most active compound in this bacterial cell-based assay, with an IC_{50} of 8 nM, much less than the IC_{50} of ∼100 nM reported for **1**, due presumably to improved cellular uptake. Substitution of one and two Cl atoms on the diphenyl ether side chain had relatively little effect on CrtM inhibition but decreased bacterial STX production by ∼3−5× (with respect to **5**) (Table 1). Shortening the $(CH_2)_n$ spacer by one CH_2 group (**14**) decreased activity in both assays (CrtM ∼40×; STX ∼400×), while lengthening the spacer by one CH_2 group (**16**) had an even larger effect (CrtM IC_{50} ∼130×, STX ∼400×, again versus **5**). We also found that replacing the diphenyl ether side chain by a biphenyl group (**10**) reduced both CrtM inhibition (by ∼20×) and STX biosynthesis (∼600×) (Table 1). So the diphenyl ethers containing a $(CH_2)_3$ spacer had the most activity, both in the enzyme and in the whole bacterial cell assays.

We next investigated the effects of changing the PO_3H_2 group to a SO_3H group (Figure 2, motif **b**) or a $-CO_2H$ group (Figure 2, motif **c**). The sulfonoacetamide (**11**) had weak activity in both assays: a $K_i = 0.81$ μM in CrtM inhibition (∼20× higher than **5**) and an $IC_{50} = 15$ μM in STX biosynthesis inhibition (∼600× higher than **5**) (Table 1). The results obtained with the carboxylic acid analogue (**21**) in which the $-PO_3H$ group was replaced with a $-CO_2H$ group were even worse, with $K_i >$ 7 μM and an IC_{50} (STX) of 200 μM, ∼200× and ∼25000× worse than with the phosphonoacetamide **5** (Table 1). So the ordering of activity is $-PO_3H_2/-PO_3^{2-} > -SO_3H/-SO_3^- \gg -CO_2H/-CO_2^-$ in both CrtM and STX biosynthesis inhibition, suggesting the likely importance of multiple electrostatic interactions (and/or H-bonding) between CrtM and the inhibitor's anionic group. Also of interest is the observation that, at least for the compounds where K_i values are accurately known (i.e., they are not limit values, Table 1), the cell-based activity values cover a larger range than do the CrtM enzyme inhibition results, suggesting the importance of variations in bacterial cell uptake between the different inhibitors.

On the basis of these observations, we next investigated the effects of methyl substitutions on activity. In the case of the **d** motif, dimethyl substitution on the acetamide CH_2 (**13**) would increase hydrophobicity, but this compound had worse CrtM activity (≳20×) and much worse (≳62500× versus **5**) activity in STX biosynthesis, where it was essentially inactive ($IC_{50} \approx$ 0.5 mM, Table 1). In the case of the N-Me substituent (Figure 2, motif **e**), the single methyl group on nitrogen (**12**) reduced activity by a factor of ∼20× versus **5** (to $K_i = 0.91$ μM), essentially the same as that seen with the dimethyl analogue **13**, but in contrast to **13**, there was still measurable STX inhibition activity ($IC_{50} = 8.6$ μM, ∼1000× worse than with **5**). That is, the N-Me (**12**) and $C(Me)_2$ (**13**) analogues have essentially the same activity in CrtM inhibition (0.91 and 0.96 μM, respectively), while STX biosynthesis inhibition is very different (8.6 and >500 μM for **12** and **13**, respectively), supporting again the idea that the $-COCH_2PO_3H_2$ group is important for cell-based activity. These results also suggested to us that the amide NH group might be important in hydrogen

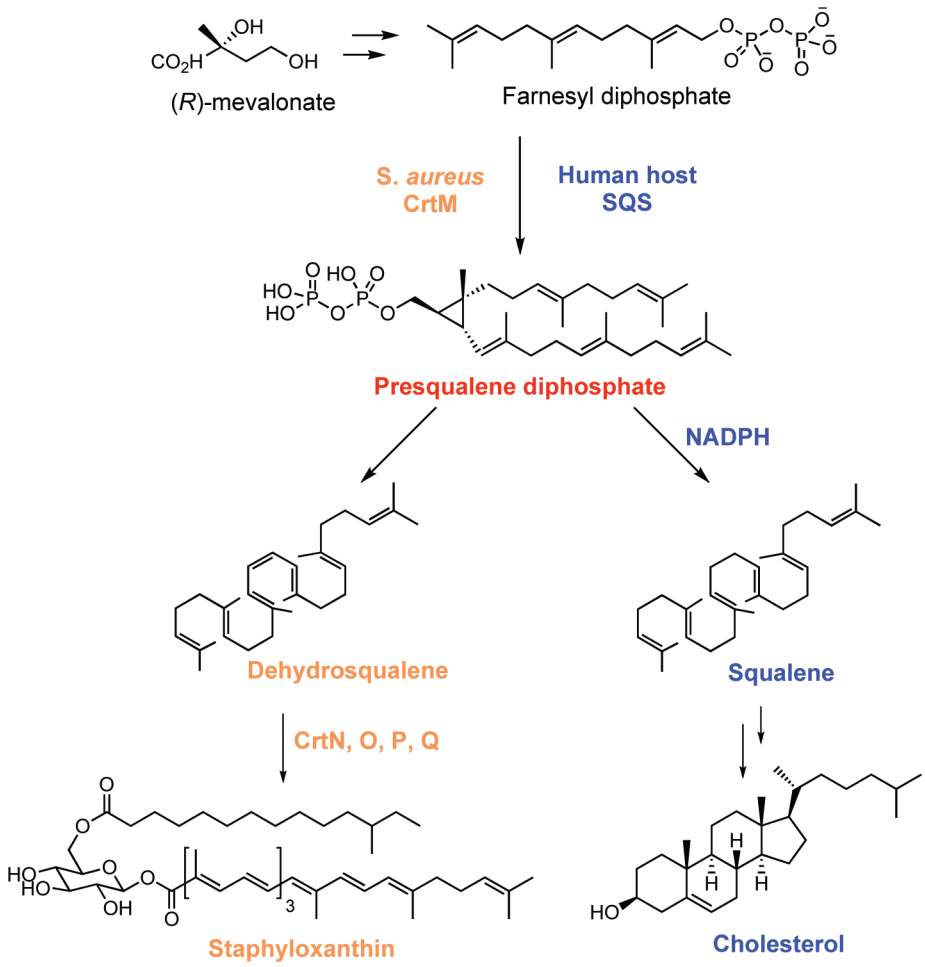

Figure 1. Schematic flowchart for staphyloxanthin and cholesterol biosynthesis from farnesyl diphosphate. The first committed step in both pathways involves the head-to-head condensation of two molecules of farnesyl diphosphate to form presqualene diphosphate, catalyzed by the CrtM enzyme in *S. aureus*, or squalene synthase in humans. In *S. aureus*, dehydrosqualene is then formed via ring-opening and elimination of diphosphate; in humans, ring-opening is accompanied by an NADPH reduction step, resulting in squalene.

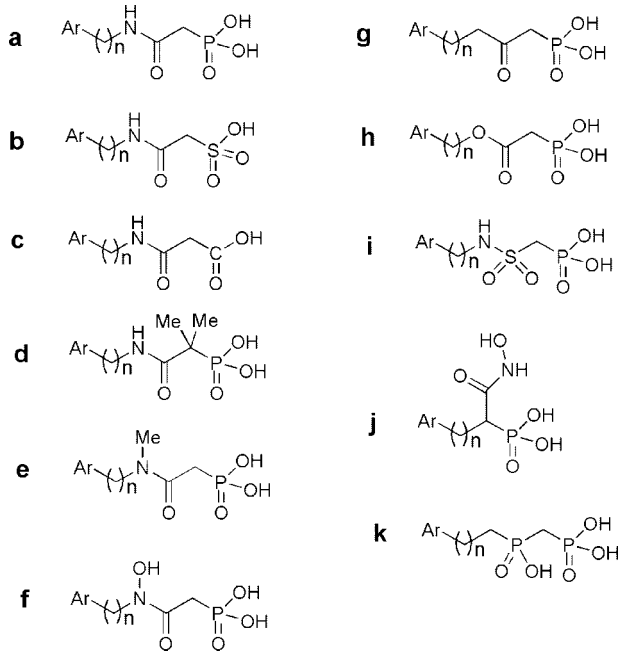

Figure 2. Structural motifs present in the different inhibitors investigated.

bonding to the protein, since the NH to NMe substitution reduced CrtM activity by ~20× (Table 1).

Given the apparent importance of this region for activity, it was of interest to see if activity might be improved by conversion of the NHCO amide moiety to a hydroxamate (NOH·CO, Figure 2, motif **f**), which would provide alternative possibilities for H-bond formation. We made three hydroxamates, **8**, **9**, and **20**, the first two species containing diphenyl ether side chains, the third, a biphenyl. Interestingly, both the dichloro and unsubstituted diphenyl ether phosphonohydroxamates had good activity in both CrtM and STX biosynthesis inhibition (Table 1), although they were both less active than the three most potent phosphonoacetamides. On average, the hydroxamates were ~6× less active against CrtM and ~2× less active in the STX biosynthesis assay (Table 1). Not unexpectedly, the biphenyl hydroxamate (**20**) was even less active, consistent with the weaker activity of the biphenyl phosphonoacetamide, **10**. So for activity, these results indicate the importance of a phosphonoacetyl group, located in either an acetamide or a hydroxamate group, suggesting the importance of both electrostatic (H-bond) interactions between the phosphonate and the protein and, most likely, hydrogen bonding between the amide (or hydroxamate) and the protein. To test these ideas further, we next investigated motifs **g**−**i**, Figure 2, using compounds **19**, **17**, and **18**. Surprisingly, the sulfonamide **19** had no activity in either the CrtM or STX biosynthesis assay (Table 1), suggesting a critical role for the amide/hydroxamate CO group as an H-bond acceptor. Consistent with this, neither

Table 1. Enzyme (CrtM, K_i), Pigment (STX, *S. aureus*, IC_{50}), and Cell Growth (IC_{50}) Inhibition Results for **4**−**21**

compound	structure	CrtM[a] Ki (μM)	STX[b] (*S. aureus*) (μM)	hSQS[c] Ki (μM)	MCF-7 cells[d] (μM)	NCI-H460 cells[e] (μM)	SF-268 cells[f] (μM)
4	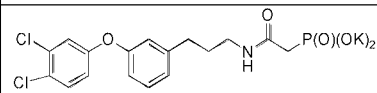	0.03	0.04	0.74	>300	>300	>300
5	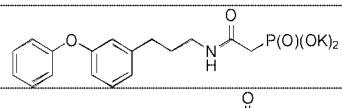	0.04	0.008	0.53	>300	>300	>300
6	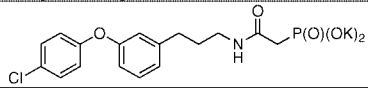	0.07	0.028	1.1	>300	>300	>300
7	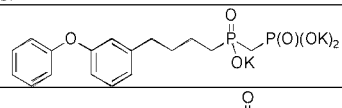	0.22	0.44	>30	>300	>300	>300
8	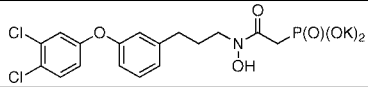	0.32	0.042	1.6	>300	>300	>300
9	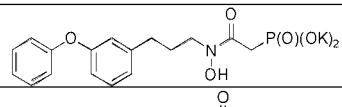	0.32	0.11	30	>300	>300	>300
10	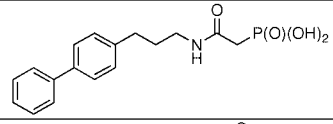	0.81	5.0	>30	>300	>300	>300
11	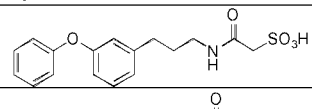	0.81	15	>30	>300	>300	>300
12	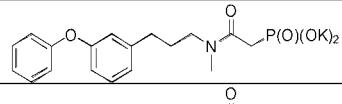	0.91	8.6	1.0	>300	>300	>300
13	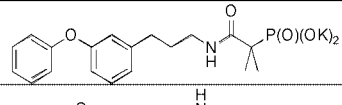	0.96	>500	0.52	>300	>300	>300
14	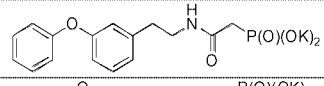	1.5	3.0	6.2	>300	>300	>300
15	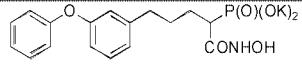	4.1	4.2	0.30	>300	>300	>300
16	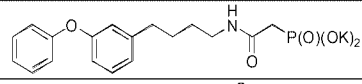	5.3	35	>30	>300	>300	>300
17	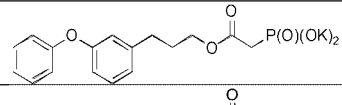	5.7	>500	>30	69	67	86
18	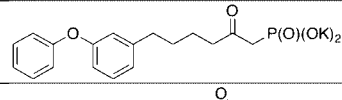	>7.0	28	20	135	130	191
19	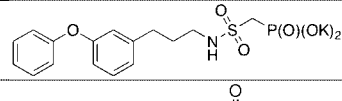	>7.0	>500	>30	>300	>300	>300
20	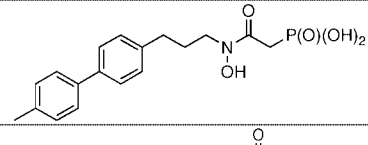	>7.0	4.1	>30	266	229	284
21	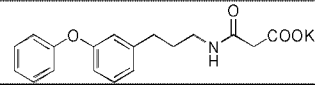	>7.0	200	>30	283	306	306

[a] The value given are the K_i values for CrtM inhibition, in μM. [b] The values given are the IC_{50} values for STX (staphyloxanthin) virulence factor inhibition in *S. aureus* and are in μM. [c] The values given are the K_i values for human squalene synthase inhibition (in vitro) and are in μM. [d] The values given are the IC_{50} values for MCF-7 cell growth inhibition, in μM. [e] The values given are the IC_{50} values for NCI-H460 cell growth inhibition, in μM. [f] The values given are the IC_{50} values for SF-268 cell growth inhibition, in μM.

the ester (**17**) nor the ketone (**18**) had significant activity in either assay (Table 1).

We then investigated two additional motifs, **j** and **k** in Figure 2. The hydroxamate (**j**, **15**) had modest activity in both assays (K_i, IC_{50} ~4 μM) but was ~100× (CrtM) to ~500× (STX) less active than was **5**. The phosphinomethylphosphonate **7** (motif **k**) was a potent CrtM inhibitor ($K_i = 220$ nM), but again we believe, due to its increased polarity, it was ~50× less effective in STX biosynthesis inhibition in whole cells than was the most potent phosphonoacetamide (**5**).

Finally, we investigated the effects of all 18 compounds on human SQS inhibition, together with their activity in growth inhibition of three human tumor cell lines (MCF-7, NCI-460, and SF-268) (Table 1). Although inhibition of human SQS may not be a particularly important toxicologic consideration, given a choice, it would seem to be preferable to have a STX biosynthesis inhibitor with poor activity against SQS, as opposed to one with potent SQS activity, and as can be seen in Table 1, several potent CrtM inhibitors do have relatively little activity in the SQS assay. More important, in essentially all cases we find no inhibition of human cell growth (in three human cell lines, $IC_{50} > 300$ μM), supporting the idea that these compounds will have low toxicity. In fact, only the ester **17** had significant activity ($IC_{50} \approx 70-90$ μM) on human cell growth, but since this compound is inactive in STX biosynthesis inhibition, it is not likely to be of interest.

Structure and Structure−Function Aspects. The results described above are of interest, since they represent the development of several new, chemically diverse virulence inhibitors for *S. aureus*. However, the relationships between structure and activity need to be explored in more detail in order to obtain a better understanding of how, in particular, the most active compounds act on their CrtM target. What is interesting about the most active compounds, the phosphonoacetamides, is that while they contain the same 3-(3-phenoxyphenyl)propyl ($PhOC_6H_4(CH_2)_3-$) side chain as found in the most active phosphonosulfonates,[18] the "backbone" is clearly about two bond lengths greater in the new compounds. So we next examined the effects of this common feature on binding.

In the CrtM enzyme, there are two binding sites for FPP,[14] and in previous work we found that phosphonosulfonates could bind to either one of these sites.[14] The diphenyl ether phosphonosulfonate **1** bound to site 1 and had interactions with 2 Mg^{2+}, while two biphenyl phosphonosulfonates (**2**, **3**) bound to site 2 with 1 and 0 Mg^{2+}, respectively. This observation complicates any QSAR analysis, since there could be 0, 1, or 2 Mg^{2+} present, and two different sites might be occupied. Plus, with the phosphonoacetamides, the presence of a longer backbone complicates the situation further, since, for example, if the diphenyl ether is located in the same region as found with **1**, the headgroup will not fit. We therefore next obtained the structure of a CrtM−**5** complex using X-ray crystallography to determine how **5** does in fact bind to CrtM, in order to provide a better, albeit qualitative, structure-based interpretation of the activity of one of the most potent inhibitors. Data collection and refinement statistics are given in Table 2, and full details are given in the Experimental Section.

CrtM crystallizes in the $P3_221$ space group, and there is one molecule per asymmetric unit. The phosphonoacetamide **5** yielded well-resolved $2F_{obs} - F_{calc}$ densities (Figure 3A), and the refined structure of **5** (red) is shown superimposed on FsPP (bound to CrtM) in Figure 3B and on **1**−**3** in Figure 3C. Interestingly, **5** binds to CrtM in a completely different manner to that observed with FsPP or any of the three phosphonosulfonates reported previously.[14] Its polar phosphonate headgroup is located in the FsPP site 1, where it makes a salt bridge with Arg45 and H-bond contacts with Gln165 and Asn168, together with a complex H-bond network with five H_2O molecules (Figure 4). However, unlike the situation found with **1**, the diphenyl ether side chain occupies the FPP site 2. In addition, the amide CO forms H-bonds with Arg45 and two H_2O molecules, and the amide NH acts as an H-bond donor to Gln165 (Figure 4B). Essentially, the increased length of **5** (over that present in the phosphonosulfonates) is accommodated in the protein by **5** "bridging" both the FPP-1 and FPP-2 binding sites (Figure 3B,C).

Table 2. Data Collection and Refinement Statistics for CrtM−**5** Complex

	CrtM−**5**
Crystal Data Collection	
radiation source	NSRRC BL13B1
wavelength (Å)	1.00000
space group	$P3_221$
unit cell dimensions	
a (Å)	80.59
b (Å)	80.59
c (Å)	90.02
resolution (Å)[a]	30−1.78 (1.84−1.78)
no. of reflections	32804 (3224)
completeness (%)	99.7 (100)
redundancy	6.3 (6.2)
R_{merge} (%)	2.6 (33.1)
$I/s(I)$	51.7 (4.6)
Refinement	
no. of reflections	31532 (2840)
R_{work} (%)	18.2 (22.9)
R_{free} (%)	21.9 (23.7)
Geometry deviations	
bond lengths (Å)	0.015
bond angles (deg)	1.6
mean *B*-values (Å^2)/no.	
protein atoms	29.5/2353
compound atoms	29.2/24
water molecules	53.1/507
Ramachandran plot (%)	
most favored	93.9
additionally allowed	6.1

[a] Values in the parentheses are for the highest resolution shells.

Given this new structure (PDB 2ZY1), it is now possible to rationalize several of the SAR observations noted above. Specifically, conversion of the $-PO_3^{2-}$ group in **5** to $-SO_3^-$ or $-CO_2^-$ can be expected to result in the loss of many of the H-bond/electrostatic interactions with Arg45, Gln165, and Asn168 and the five H_2O molecules. Second, conversion of the amide NH to NMe will prevent H-bond formation with Gln165, as will formation of an ester (**17**) or a ketone (**18**) in this region. Likewise, conversion of the amide to the hydroxamate (**9**) results in disruption of this H-bond interaction which may, however, be partially compensated for by other conformational changes, since **9** still retains quite good ($K_i = 320$ nM) CrtM activity. But how can we correlate our enzyme inhibition results with cell based inhibition of STX biosynthesis, something that is clearly desirable because we are interested in good inhibition of virulence factor formation in cells and not just good CrtM inhibitors (which might not actually get into cells)?

In Vitro and in Vivo Results. When considering all compounds investigated, we find that there is quite a good correlation between the CrtM enzyme pK_i ($= -\log_{10} K_i$, M)

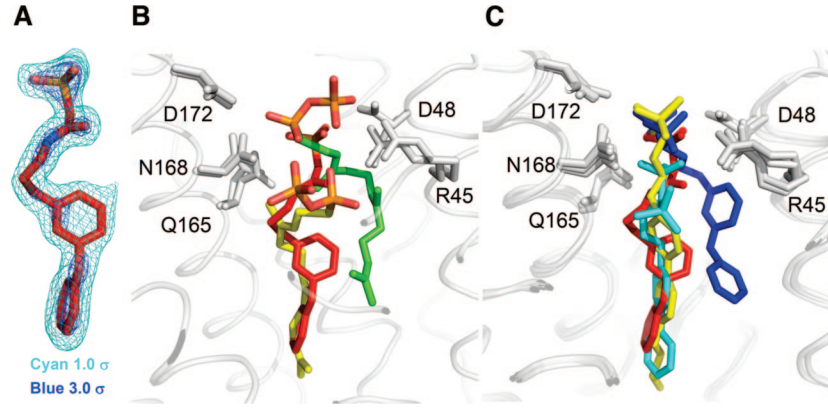

Figure 3. X-ray crystallographic results: (A) electron density for **5** in CrtM; (B) superposition of **5** (red) in the CrtM active site (2ZY1) with that of two molecules (green, yellow) of *S*-thiolofarnesyl diphosphate (2ZCP); (C) superposition of **5** (red) with **1** (blue), **2** (yellow), **3** (cyan) in the CrtM active site (2ZCQ, 2ZCR, 2ZCS).

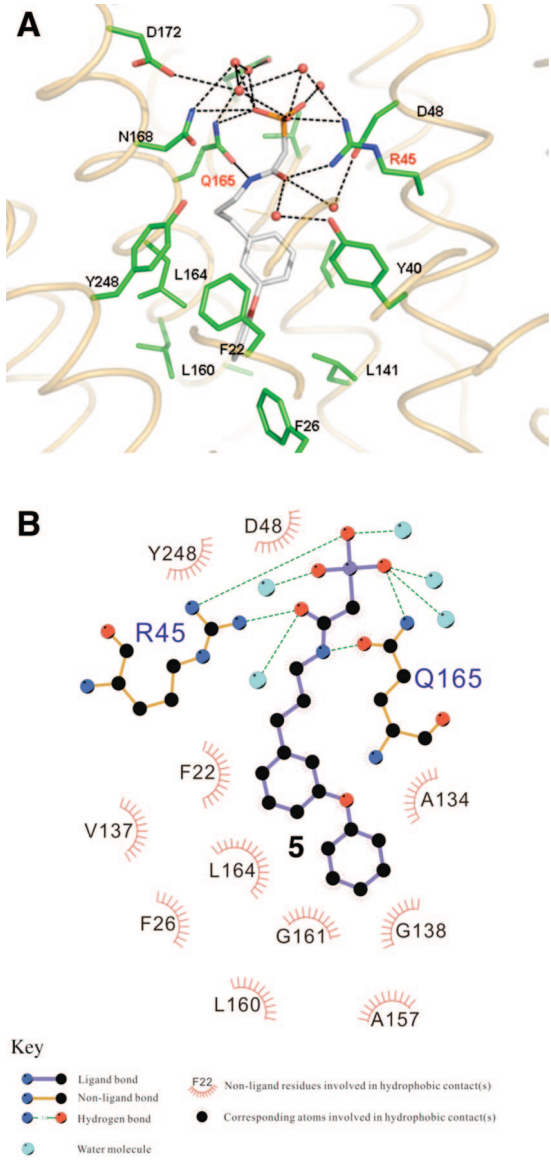

Figure 4. Interactions between **5** and different residues in the CrtM active site: (A) Pymol[26] view; (B) Ligplot[27] interactions.

and cell STX biosynthesis inhibition pIC_{50} ($= -\log_{10} IC_{50}$, M) values, as can be seen in Figure 5A where the R^2 value is 0.73 (for the 14 compounds having nonlimit K_i/IC_{50} values). However, when we add results for the 36 compounds reported

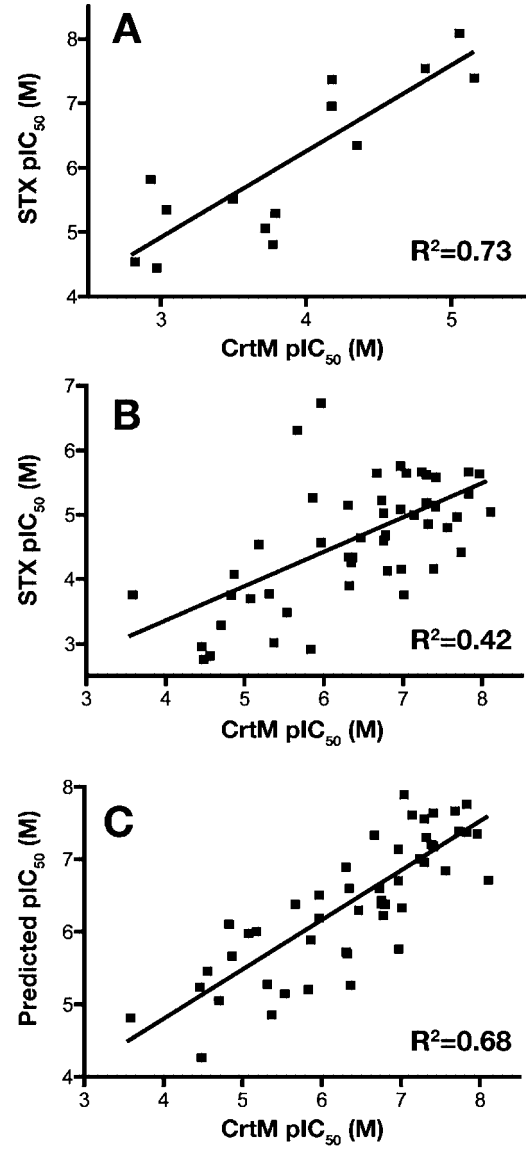

Figure 5. Figure showing correlations between CrtM inhibition and STX biosynthesis inhibition: (A) data for the 14 compounds reported in this work; (B) combination of 36 phosphonosulfonate inhibitor results (ref 18) with the 14 compounds reported here; (C) combinatorial descriptor search result for all 50 compounds tested (here and in ref 18) in CrtM and STX biosynthesis inhibition. The lower R^2 value in part B is likely due the high diversity of the large data set; the R^2 improves to 0.68 by using the combinatorial descriptor approach.[19]

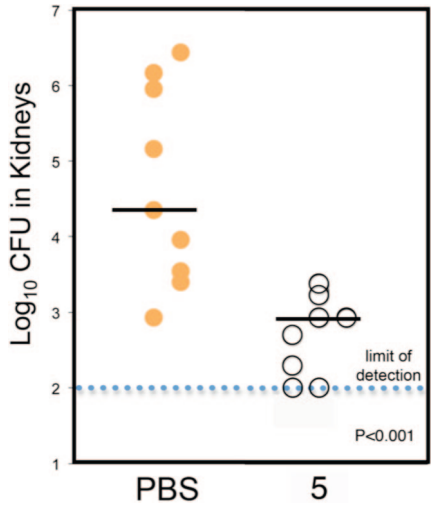

Figure 6. In vivo results showing ~96% reduction in *S. aureus* colony formation in mice receiving treatment with **5**.

previously to the correlation, the $n = 50$ compound data set exhibits a much worse correlation (Figure 5B) with an $R^2 = 0.42$. This is similar to the results we reported previously where we found for 10 different enzyme/cell assays that on average the R^2 value for the pK_i/pIC_{50} correlation was only 0.32 (ref 19), making any predictions of cell-based activity, based on enzyme activity, in some cases, impossible. The large discrepancies found were, we proposed, likely to be due to the neglect of factors that affect inhibitor uptake into cells, and we described a general method in which this aspect might be taken into consideration, by using a "combinatorial descriptor approach".[19] That is, we described cell activity by using the following equation:

$$pIC_{50}(\text{cell}) = apK_i(\text{enzyme}) + bB + cC + d$$

where $a-d$ are linear regression coefficients and where B and C are mathematical descriptors (such as SlogP) chosen in a combinatorial manner from a large series of potential descriptors (such as the 230 descriptors in the program MOE[20]). Applying this same method to the combined data set (50 compounds), we now obtain (Figure 5C) $R^2 = 0.68$, a significant improvement.

To investigate in vivo activity, we selected the most potent in vitro STX biosynthesis inhibitor (**5**) and carried out an intraperitoneal challenge experiment with *S. aureus* in exactly the same manner as reported previously for **1**.[14] We treated one group of mice ($n = 9$) with 0.5 mg of **5** twice per day (days −1, 0, 1, and 2) and a second group ($n = 9$) with equivalent volume injections of PBS control. Upon sacrificing the mice at 72 h, *S. aureus* bacterial counts in the kidneys of the mice treated with **5** were significantly lower than those of the control group ($p < 0.001$). The median number of colony forming units (cfu) in the untreated animals was 22 500 cfu/mL compared with 850 cfu/mL for the treated animals (Figure 6), about a 96% reduction in surviving bacteria in the treatment group.

Synthetic Aspects. We outline here the synthetic schemes used to prepare **4**−**21**; full protocols for each compound are given in the Experimental Section. A general synthetic route to the most active phosphonoacetamide and *N*-hydroxyacetamide (hydroxamate) compounds is shown in Scheme 1. The reaction of aldehyde **24** and sodium diethyl cyanomethylphosphonate in THF gave, after hydrogenation, compound **25** in almost quantitative yield, which after reduction with 2 equiv of $LiAlH_4$ and $AlCl_3$ afforded amine **26**. Amine **26** was then reacted with dibenzylphosphonoacetic acid **22** in the presence of the coupling reagent *N*-ethyl-*N*′-(3-dimethylaminopropyl)carbodiimide (EDC) to give, after hydrogenation to remove the benzyl groups, a phosphonoacetamide (e.g., **5**). *N*-Hydroxyphosphonoacetamide compounds, such as **9**, were prepared from substituted hydroxylamine **29** and diethylphosphonoacetyl chloride **23**, after hydrolysis with TMSBr (to remove ethyl phosphono-esters) and hydrogenation (to remove *O*-benzyl protecting group), also shown in Scheme 1. Compounds **13**, **11**, **17**, **21**, **14**, and **16** were made similarly, with a carbodiimide mediated amide/ester formation reaction as the main step, as shown in Scheme 2.

Other compounds were made as outlined in Scheme 3. Compound **15** is an analogue of **5** but has a hydroxamate group in its side chain. Alkylation of ethyl dibenzylphosphonoacetate with iodide **28** gave compound **30**, as shown in Scheme 3. The carboxylate ethyl ester was then selectively hydrolyzed (1 M KOH) and the corresponding acid coupled with *O*-benzylhydroxylamine under standard carbodiimide conditions, followed by hydrogenation to remove three benzyl protecting groups, to give **15**. Compound **18** is a β-ketophosphonate analogue of **5**, and its synthesis began with a Suzuki coupling reaction of an ethyl 4-pentenoate derived boron compound and 4-bromodiphenyl ether (Scheme 3), affording carboxylate ester **31**. Compound **31** was then reacted with 2 equiv of lithium diethyl methylphosphonate at −78 °C to give, after TMSBr mediated hydrolysis, **18**. The reaction of precursor amine **26** with methanesulfonyl chloride produced methylsulfamide **32** (Scheme 3). This was then treated with 2 equiv of butyllithium to give a dianion, which was reacted with diethyl chlorophosphate and hydrolyzed with TMSBr, resulting in the phosphonosulfamide **19**. Compound **7** was made by an alkylation reaction of the dianion of triethyl methylphosphinomethylphosphonate with iodide **28**, followed by hydrolysis.

Conclusions

The results we have described here are of interest for a number of reasons. First, we have synthesized a broad variety of inhibitors of the dehydrosqualene synthase enzyme, CrtM, exhibiting novel structural motifs. Second, we have determined their activity in CrtM inhibition and in staphyloxanthin biosynthesis in *S. aureus*. Third, we show that STX biosynthesis activity for a broad range of inhibitors can be predicted from enzyme inhibition results with quite good R^2 values by using a combinatorial descriptor approach. Fourth, we have demonstrated that the most potent STX biosynthesis inhibitor in vitro also has activity in vivo in preventing infection. Fifth, we show that these compounds have no activity against three human cell lines. Sixth, we have obtained the X-ray crystallographic structure of the most potent STX biosynthesis inhibitor investigated here (**5**) bound to CrtM. The structure is unusual in that the inhibitor actually bridges the FPP-1 and FPP-2 sites observed previously,[14] whereas the phosphonosulfonates reported previously bind to one or other of these sites but not to both. Many of the major changes in CrtM activity between the different motifs investigated can be interpreted in terms of the crystallographic results, opening up the way to the further development of this class of compound as novel anti-infective agents targeting inhibition of the biosynthesis of the staphyloxanthin virulence factor in *S. aureus*.

Experimental Section

General Synthesis Methods. General Method A. Triethyl phosphonoacetate, or diethyl cyanomethylphosphonate (3.3

Scheme 1. General Synthetic Routes to Phosphonoacetamides and *N*-Hydroxyphosphonoacetamides[a]

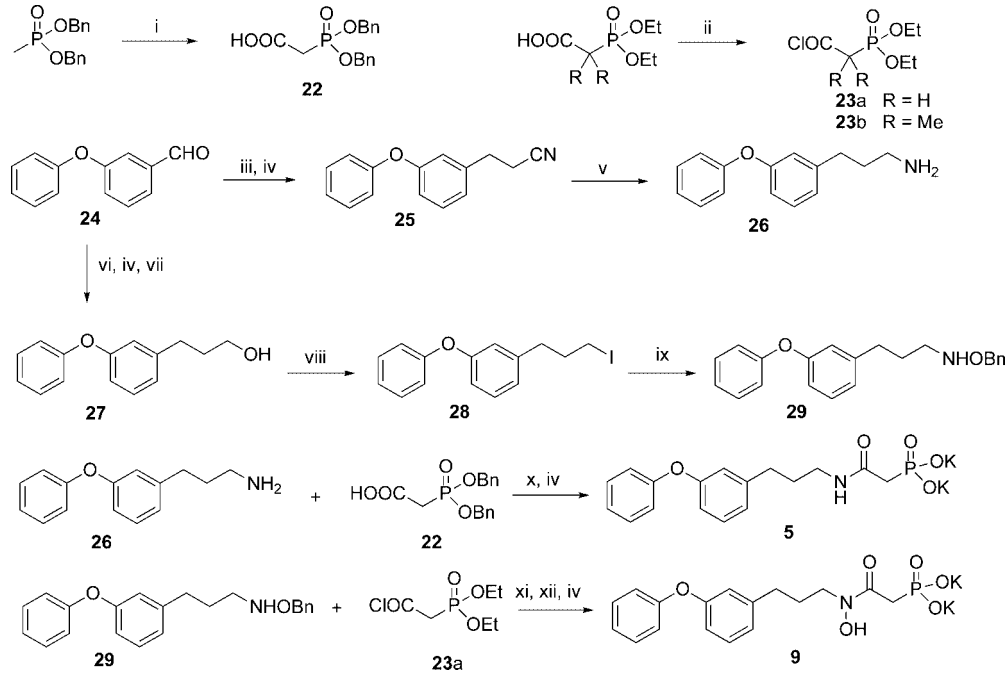

[a] Reagents and conditions: (i) BuLi, then CO_2, −78 °C, 63%; (ii) oxalyl chloride (2 equiv), 100%; (iii) NaH, diethyl cyanomethylphosphonate; (iv) H_2, Pd/C (5%); (v) $LiAlH_4$ (2 equiv), $AlCl_3$ (2 equiv); (vi) NaH, triethyl phosphonoacetate; (vii) $LiAlH_4$ (2 equiv); (viii) MsCl, NEt_3, then NaI (5 equiv); (ix) *O*-benzylhydroxylamine (2 equiv), diisopropylethylamine, DMF, 80 °C, 50% overall from 24; (x) EDC, HOBt; (xi) NEt_3; (xii) TMSBr (2 equiv), then MeOH.

Scheme 2[a]

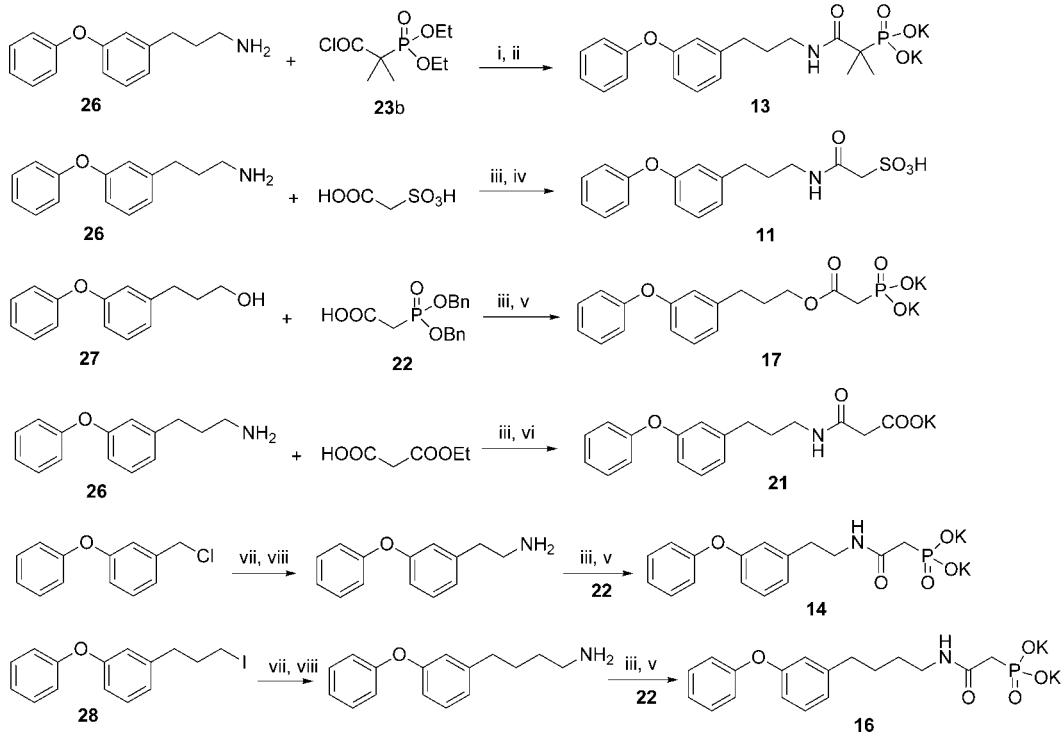

[a] Reagents and conditions: (i) NEt_3; (ii) TMSBr (2 equiv), then MeOH, 48% for two steps; (iii) EDC, HOBt; (iv) DOWEX ion-exchange resin, H^+ form, 85% for two steps; (v) H_2, Pd/C (5%); (vi) KOH, MeOH/H_2O, 66% for two steps; (vii) NaCN, DMF; (viii) $LiAlH_4$ (2 equiv), $AlCl_3$ (2 equiv).

mmol), was added dropwise to NaH (145 mg, 60% in oil, 3.6 mmol) suspended in dry THF (7 mL) at 0 °C. To the resulting clear solution was added a benzaldehyde (3 mmol), and after being stirred at room temperature for 0.5 h, the reaction mixture was partitioned between diethyl ether (50 mL) and water (50 mL). The organic layer was dried and evaporated. The oily residue was then hydrogenated in MeOH (15 mL) in the presence of 5% Pd/C (50 mg). The catalyst was filtered and the filtrate concentrated and dried in vacuo.

General Method B. The nitrile (or ester) obtained using general method A was added slowly to 2 equiv of $LiAlH_4/AlCl_3$, or $LiAlH_4$, in dry THF at 0 °C. After the mixture was stirred at room temperature for 2 h, the reaction was carefully quenched by adding a few drops of water and the reaction mixture filtered and evaporated.

Scheme 3[a]

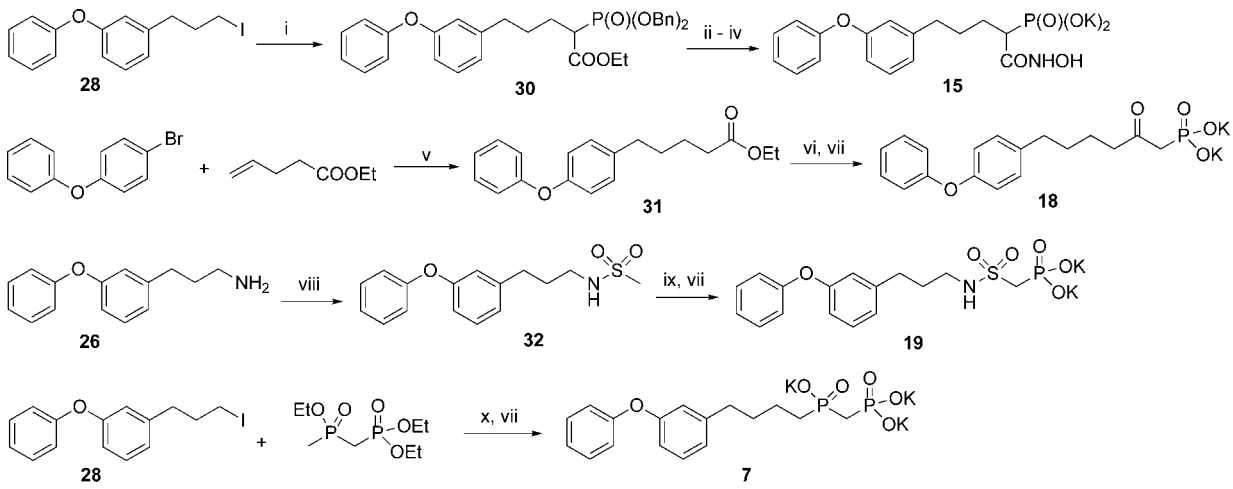

[a] Reagents and conditions: (i) NaH, ethyl dibenzylphosphonoacetate, 68%; (ii) KOH, MeOH/H_2O; (iii) *O*-benzylhydroxylamine, EDC, HOBt; (iv) H_2, Pd/C (5%), 31% from 30; (v) 9-BBN, then $Pd(PPh_3)_4$, K_3PO_4, 80 °C, 48%; (vi) diethyl methylphosphonate (2 equiv), BuLi, −78 C, 65%; (vii) TMSBr, then MeOH; (viii) MsCl, NEt_3; (ix) BuLi (2 equiv), −78 °C, then diethyl chlorophosphate, 76%; (x) BuLi (2 equiv), −78 °C, then **28**, 58%.

General Method C. To a solution of a carboxylic acid (1 mmol) and an amine (1 mmol) in CH_2Cl_2 (5 mL) were added *N*-ethyl-*N*′-(3-dimethylaminopropyl)carbodiimide (EDC) (1.5 mmol) and 1-hydroxybenzotriazole (1 mmol). After the mixture was stirred for 2 h at room temperature, 50 mL of ethyl acetate was added and the reaction mixture washed successively with 1 N HCl (5 mL), water (5 mL), and saturated $NaHCO_3$ (5 mL), dried, and evaporated. The amide was purified using flash chromatography (silica gel, ethyl acetate).

General Method D. A DMF solution (3 mL) containing a halide (3 mmol), *O*-benzylhydroxylamine (6 mmol) and diisopropylethylamine (3 mmol) was heated at 90 °C for 24 h. After the mixture was cooled, diethyl ether (50 mL) was added and the mixture was washed with H_2O (20 mL), dried, and evaporated. The alkylated hydroxylamine, such as **29**, was purified by using column chromatography (silica gel; hexane/ethyl acetate, 6/1).

General Method E. To a diethyl phosphonate (1 mmol) in dry CH_3CN (3 mL) was added TMSBr (2 mmol) at room temperature. After 6 h, the solution was evaporated and methanol (5 mL) added. Neutralization with 1 N KOH to pH 8, followed by evaporation to dryness and triturating with acetone, gave a white powder.

All reagents used were purchased from Aldrich (Milwaukee, WI). The purities of all compounds were routinely monitored by using ^1H and ^{31}P NMR spectroscopy at 400 or 500 MHz on Varian (Palo Alto, CA) Unity spectrometers. All compounds were of ≥95% purity, as determined by combustion analysis. The details of these syntheses are as follows.

Diethylphosphonoacetyl Chloride (23a). Compound **23a** was prepared by mixing diethylphosphonoacetic acid (1.5 mmol) with oxalyl chloride (3 mmol) in benzene (5 mL) in the presence of one drop of DMF for 1 h, followed by evaporation. The oily residue was used immediately for the next reaction.

3-(3-Phenoxyphenyl)propyl Iodide (28). Alcohol **27**, obtained from 3-phenoxybenzaldehyde (3 mmol) following general methods A and B, in CH_2Cl_2 (10 mL) containing NEt_3 (0.5 mL, 3.6 mmol) was reacted with methanesulfonyl chloride (230 μL, 3 mmol) at 0 °C. After 1 h, diethyl ether (50 mL) and water (50 mL) were added and the organic layer was collected, washed with 1 N HCl and saturated $NaHCO_3$, dried, and evaporated to dryness. The oily residue was treated with NaI (1.35 g, 9 mmol) in acetone (7 mL) at 60 °C for 1 h. The reaction mixture was then partitioned between diethyl ether (50 mL) and water (50 mL) and the organic layer washed with 5% $Na_2S_2O_3$, dried, and evaporated to dryness to give iodide **28**. The iodide thus obtained is quite pure, according to ^1H and ^{13}C NMR spectra, and may be used in the next step without further purification.

***N*-[3-(3-(3,4-Dichlorophenoxy)phenyl)propyl]phosphonoacetamide Dipotassium Salt (4).** 3-(3-(3,4-Dichlorophenoxy)phenyl)-propylamine was prepared from 3-(3,4-dichlorophenoxy)benzaldehyde (1 mmol), using general method A, and was then coupled with dibenzylphosphonoacetic acid according to general method C to give the dibenzyl ester of **4**. The benzyl groups were removed by catalytic hydrogenation (5% Pd/C in methanol for 1 h) followed by neutralization with KOH to give compound **4** as a white powder (245 mg, 48% overall yield). Anal. ($C_{17}H_{16}Cl_2K_2NO_5P\cdot0.5CH_3OH$) C, H, N. ^1H NMR (400 MHz, D_2O): δ 1.60−1.70 (m, 2H, CH_2); 2.35 (d, J = 20 Hz, 2H, CH_2P); 2.46 (t, J = 7.6 Hz, 2H, $PhCH_2$); 2.98 (t, J = 7.2 Hz, 2H, CH_2N); 6.70−7.30 (m, 7H, aromatic). ^{31}P NMR (D_2O): δ 13.6.

***N*-[3-(3-Phenoxyphenyl)propyl]phosphonoacetamide Dipotassium Salt (5).** Amine **26** was prepared from 3-phenoxybenzaldehyde (1 mmol) using general method A and was then coupled with dibenzylphosphonoacetic acid according to general method C to give the dibenzyl ester of **5**. The benzyl groups were removed by hydrogenation for 1 h, catalyzed with 5% Pd/C in methanol, followed by neutralization with KOH to give compound **5** as a white powder (307 mg, 62% overall yield). Anal. ($C_{17}H_{18}K_2NO_5P\cdot1.5H_2O$) C, H, N. ^1H NMR (400 MHz, D_2O): δ 1.60−1.70 (m, 2H, CH_2); 2.35 (d, J = 20 Hz, 2H, CH_2P); 2.46 (t, J = 7.6 Hz, 2H, $PhCH_2$); 2.98 (t, J = 7.2 Hz, 2H, CH_2N); 6.70−7.30 (m, 9H, aromatic). ^{31}P NMR (D_2O): δ 13.7.

***N*-[3-(3-(4-Chlorophenoxy)phenyl)propyl]phosphonoacetamide Dipotassium Salt (6). 6** was prepared in the same way as **5**, but using 3-(4-chlorophenoxy)benzaldehyde (1 mmol) as starting material, as a white powder (267 mg, 58% overall yield). Anal. ($C_{17}H_{17}ClK_2NO_5P\cdot0.3KCl\cdot1.5H_2O$) C, H, N. ^1H NMR (400 MHz, D_2O): δ 1.60−1.70 (m, 2H, CH_2); 2.37 (d, J = 20 Hz, 2H, CH_2P); 2.49 (t, J = 7.6 Hz, 2H, $PhCH_2$); 3.01 (t, J = 7.2 Hz, 2H, CH_2N); 6.70−7.30 (m, 8H, aromatic). ^{31}P NMR (D_2O): δ 13.5.

3-(3-Phenoxyphenyl)propylphosphinylmethylphosphonic Acid Tripotassium Salt (7). Triethyl methylphosphinylmethylphosphonate (1 mmol) was treated with BuLi (2.2 mmol) in THF at −78 °C for 1 h, followed by addition of iodide **28** (1.1 mmol). The reaction mixture was allowed to warm to room temperature over 3 h and was then quenched with saturated NH_4Cl. The product was purified with column chromatography (silica gel; ethyl acetate/methanol, 20/1) and deprotected using general method E to give **7** as a white powder (320 mg, 62% overall yield). Anal. ($C_{17}H_{19}K_3O_6P_2\cdot H_2O$) C, H. ^1H NMR (400 MHz, D_2O): δ 1.30−1.60 (m, 6H, $3CH_2$); 1.75−1.85 (m, 2H, CH_2P); 2.43 (t, J = 7.6 Hz, 2H, $PhCH_2$); 6.70−7.30 (m, 9H, aromatic). ^{31}P NMR (D_2O): δ 16.3 (s, 1P); 39.9 (s, 1P).

***N*-Hydroxy-*N*-[3-(3-(3,4-dichlorophenoxy)phenyl)propyl]phosphonoacetamide Dipotassium Salt (8). 8** was prepared in the same way as **9**, but using 3-(3,4-dichlorophenoxy)benzaldehyde (3 mmol) as starting material, as a white powder (428 mg, 28% overall yield).

Anal. ($C_{17}H_{16}Cl_2K_2NO_6P\cdot KBr$) C, H, N. ^{1}H NMR (400 MHz, D_2O): δ 1.75−1.85 (m, 2H, CH_2); 2.48 (t, J = 7.6 Hz, 2H, $PhCH_2$); 2.63 (d, J = 20 Hz, 2H, CH_2P); 3.46 (t, J = 7.2 Hz, 2H, CH_2N); 6.70−7.35 (m, 7H, aromatic). ^{31}P NMR (D_2O): δ 15.6.

***N*-Hydroxy-*N*-[3-(3-phenoxyphenyl)propyl]phosphonoacetamide Dipotassium Salt (9).** General method D with iodide **28** gave substituted hydroxylamine **29** (1 mmol), which was reacted with the acid chloride in the presence of NEt_3 (2 mmol) in CH_2Cl_2 (5 mL) at 0 °C. After the mixture was stirred for 1 h, the coupling product was purified by using column chromatography (silica gel, ethyl acetate) and was then deprotected following general method E. Hydrogenation (5% Pd/C, MeOH) gave compound **9** as a white powder (312 mg, 56% overall yield). ^{1}H NMR (400 MHz, D_2O): δ 1.65−1.75 (m, 2H, CH_2); 2.42 (t, J = 7.6 Hz, 2H, $PhCH_2$); 2.66 (d, J = 20 Hz, 2H, CH_2P); 3.39 (t, J = 7.2 Hz, 2H, CH_2N); 6.70−7.20 (m, 9H, aromatic). ^{31}P NMR (D_2O): δ 15.8.

***N*-[3-(4-Biphenyl)propyl]phosphonoacetamide (10).** 3-(4-Biphenyl)propylamine was prepared from 4-phenylbenzaldehyde (1 mmol), using general method A, and was then coupled with dibenzylphosphonoacetic acid according to general method C to give the dibenzyl ester of **10**. The benzyl groups were removed by hydrogenation (catalyzed with 5% Pd/C in methanol) for 1 h, followed by neutralization with KOH, to give compound **10** as a white powder (222 mg, 65% overall yield). Anal. ($C_{17}H_{20}K_2NO_4P\cdot 0.25CH_3OH$) C, H, N. ^{1}H NMR (400 MHz, D_2O): δ 1.65−1.75 (m, 2H, CH_2); 2.31 (d, J = 20 Hz, 2H, CH_2P); 2.55 (t, J = 7.6 Hz, 2H, $PhCH_2$); 3.03 (t, J = 7.2 Hz, 2H, CH_2N); 7.20−7.55 (m, 9H, aromatic). ^{31}P NMR (D_2O): δ 12.8.

***N*-[3-(3-Phenoxyphenyl)propyl]sulfoacetamide (11).** Amine 26 (1 mmol) was coupled with sulfoacetic acid (1 mmol) according to general method C (without addition of 1-hydroxybenzotriazole) to give **11**. The product was purified by using column chromatography (DOWEX ion-exchange resin, H^+ form, methanol as eluent) as an off-white powder (315 mg, 85% overall yield). Anal. ($C_{17}H_{19}NO_5S$) C, H, N. ^{1}H NMR (400 MHz, D_2O): δ 1.60−1.70 (m, 2H, CH_2); 2.44 (m, 2H, $PhCH_2$); 3.02 (m, 2H, CH_2N); 3.59 (s, 2H, CH_2S); 6.70−7.30 (m, 9H, aromatic).

***N*-Methyl-*N*-[3-(3-phenoxyphenyl)propyl]phosphonoacetamide Dipotassium Salt (12).** Amine **26** (1 mmol) was reacted with benzyl chloroformate (ZCl, 1 mmol) in the presence of NEt_3 to give Z-protected amine **26** which was then methylated in THF with MeI (1.5 equiv) and NaH (1.2 equiv) overnight. After hydrogenation (5% Pd/C in MeOH) to remove the Z-protecting group, the N-methylated amine **5** was coupled with dibenzylphosphonoacetic acid, according to general method B, to give the dibenzyl ester of **12**. The benzyl groups were removed by hydrogenation (5% Pd/C in methanol) for 1 h, followed by neutralization with KOH to give compound **12** as a white powder (220 mg, 50% overall yield). Anal. ($C_{18}H_{20}K_2NO_5P$) C, H, N. The NMR spectrum of **12** showed that two rotamers (with respect to the amide bond) exist with ratio of ~45:55. ^{1}H NMR (400 MHz, D_2O): δ 1.60−1.80 (m, 2H, CH_2); 2.35−2.45 (m, 2H, CH_2P); 2.45−2.95 (m, 5H, Me and $PhCH_2$); 3.10−3.40 (m, 2H, CH_2N); 6.80−7.30 (m, 9H, aromatic). ^{31}P NMR (D_2O): δ 13.6.

***N*-[3-(3-Phenoxyphenyl)propyl]phosphonodimethylacetamide Dipotassium Salt (13).** Diethyl phosphonodimethylacetate (3 mmol) was treated with 3 N KOH (5 mL) in ethanol (8 mL) for 24 h, followed by acidifiction with HCl to give the corresponding carboxylic acid. As with compound **23a**, the acid was then converted to the acid chloride **23b**, which was reacted with 1 equiv of amine **26** in the presence of NEt_3 in CH_2Cl_2 (5 mL) at 0 °C. After the mixture was stirred for 1 h, the coupling product was purified by using column chromatography (silica gel, ethyl acetate) and was then deprotected following general method E to give **13** as a white powder (335 mg, 21% overall yield). Anal. ($C_{19}H_{22}K_2NO_5P\cdot 0.5KBr\cdot H_2O$) C, H, N. ^{1}H NMR (400 MHz, D_2O): δ 1.09 (d, J = 13.6 Hz, 6H, $2CH_3$); 1.60−1.70 (m, 2H, CH_2); 2.46 (m, 2H, $PhCH_2$); 2.99 (m, 2H, CH_2N); 6.85−7.25 (m, 9H, aromatic). ^{31}P NMR (D_2O): δ 22.9.

***N*-[2-(3-Phenoxyphenyl)ethyl]phosphonoacetamide Dipotassium Salt (14).** 3-Phenoxybenzyl chloride (2 mmol) and NaCN (2.2 mmol) were stirred in DMF (2 mL) overnight at 60 °C. After the mixture was cooled, diethyl ether (50 mL) was added and the mixture was washed with water and the organic layer dried and evaporated. 2-(3-Phenoxyphenyl)ethylamine was prepared from the nitrile so obtained, using general method B, and was then coupled with dibenzylphosphonoacetic acid according to general method C to give the dibenzyl ester of **14**. The benzyl groups were removed by catalytic hydrogenation (5% Pd/C in methanol for 1 h) followed by neutralization with KOH to give compound **14** as a white powder (387 mg, 45% overall yield). Anal. ($C_{16}H_{16}K_2NO_5P\cdot H_2O$) C, H, N. ^{1}H NMR (400 MHz, D_2O): δ 2.39 (d, J = 20 Hz, 2H, CH_2P); 2.58 (t, J = 7.6 Hz, 2H, $PhCH_2$); 3.05 (t, J = 7.2 Hz, 2H, CH_2N); 6.70−7.30 (m, 9H, aromatic). ^{31}P NMR (D_2O): δ 13.8.

***N*-Hydroxy-2-phosphono-5-(3-phenoxyphenyl)pentamide Dipotassium Salt (15).** Iodide **28** was added to a cold DMF solution containing ethyl dibenzylphosphonoacetate (1 equiv) and NaH (1.1 equiv). After the mixture was stirred for 3 h at room temperature, the product **30** was purified by using column chromatography (silica gel; hexane/ethyl acetate, 1/1). **30** was then treated with 3 N KOH in EtOH/H_2O (3:1) for 24 h and the resulting solution was reduced in volume and then acidified with 3 N HCl, to give the corresponding carboxylic acid. The acid so obtained was reacted with *O*-benzylhydroxylamine, according to general method C, to give protected **15**, which was then hydrogenated in the presence of 5% Pd/C in MeOH for 1 h to afford, after neutralization with KOH, **15** as a white powder (293 mg, 21% overall yield). Anal. ($C_{17}H_{18}K_2NO_6P\cdot 0.5C_2H_5OH$) C, H, N. ^{1}H NMR (400 MHz, D_2O): δ 1.25−1.75 (m, 4H, CH_2); 2.20−2.50 (m, 3H, CH + $PhCH_2$); 6.70−7.25 (m, 9H, aromatic). ^{31}P NMR (D_2O): δ 17.5.

***N*-[4-(3-Phenoxyphenyl)butyl]phosphonoacetamide Dipotassium Salt (16).** Iodide **28** (2 mmol) and NaCN (2.2 mmol) were stirred in DMF (2 mL) overnight at 60 °C. After the mixture was cooled, diethyl ether (50 mL) was added and the mixture washed with water and the organic layer evaporated. 4-(3-Phenoxyphenyl)butylamine was prepared from the nitrile so obtained, using general method B, and was then coupled with dibenzylphosphonoacetic acid, according to general method C, to give the dibenzyl ester of **16**. The benzyl groups were removed by catalytic hydrogenation (5% Pd/C in methanol for 1 h) followed by neutralization with KOH to give compound **16** as a white powder (475 mg, 51% overall yield). Anal. ($C_{18}H_{20}K_2NO_5P\cdot 1.5H_2O$) C, H, N. ^{1}H NMR (400 MHz, D_2O): δ 1.55−1.70 (m, 4H, CH_2); 2.39 (d, J = 20 Hz, 2H, CH_2P); 2.48 (t, J = 7.6 Hz, 2H, $PhCH_2$); 3.01 (t, J = 7.2 Hz, 2H, CH_2N); 6.70−7.30 (m, 9H, aromatic). ^{31}P NMR (D_2O): δ 13.5.

3-(3-Phenoxyphenyl)propyl Phosphonoacetate Dipotassium Salt (17). Alcohol **27** was coupled with dibenzylphosphonoacetic acid according to general method C to give dibenzyl ester of **17**. The benzyl groups were removed by catalytic hydrogenation (5% Pd/C in methanol for 1 h) followed by neutralization with KOH to give compound **17** as a white powder (180 mg, 42% overall yield). Anal. ($C_{17}H_{17}K_2O_6P$) C, H. ^{1}H NMR (400 MHz, D_2O): δ 1.60−1.70 (m, 2H, CH_2); 2.38 (d, J = 20 Hz, 2H, CH_2P); 2.44 (t, J = 7.6 Hz, 2H, $PhCH_2$); 3.47 (t, J = 7.2 Hz, 2H, CH_2O); 6.70−7.30 (m, 9H, aromatic). ^{31}P NMR (D_2O): δ 13.9.

2-Oxo-6-(4-phenoxyphenyl)hexylphosphonic Acid Dipotassium Salt (18). 9-BBN (0.5 M in THF, 9 mL) was added to ethyl 4-pentenoate (3 mmol) at 0 °C and the reaction mixture stirred at room temperature for 2 h. 4-Bromodiphenylether (3 mmol), $Pd(PPh_3)_4$ (0.15 mmol), K_3PO_4 (6 mmol), and H_2O (2 mL) were then added, and the reaction mixture was refluxed overnight. The organic layer was evaporated and purified by using column chromatography (silica gel; hexane/ether, 6/1) to afford ester **31**, which was then reacted with 2 equiv of the lithium salt of diethyl methylphosphonate at −78 °C, for 2 h. The reaction was quenched with saturated NH_4Cl, diethyl ether added to extract the product, and the organic solvent removed. The oily residue was purified by using column chromatography (silica gel, ethyl acetate) and deprotected according to general method E to give compound **18**

as a white powder (312 mg, 20% overall yield). Anal. ($C_{18}H_{19}K_2O_5P \cdot 0.5KBr \cdot 2H_2O$) C, H. ^{1}H NMR (400 MHz, D_2O): δ 1.30−1.50 (m, 4H, CH_2); 2.44 (t, J = 7.6 Hz, 2H, $PhCH_2$); 2.54 (t, J = 7.6 Hz, 2H, CH_2CO); 2.70 (d, J = 20 Hz, 2H, CH_2P); 6.80−7.25 (m, 9H, aromatic). ^{31}P NMR (D_2O): δ 11.0.

***N*-[3-(3-Phenoxyphenyl)propyl]phosphonomethylsufamide Dipotassium Salt (19).** Amine **26** prepared from 3-phenoxybenzaldehyde (3 mmol) using general method A was reacted with 1 equiv of methanesulfonyl chloride in CH_2Cl_2 in the presence of 1.2 equiv of NEt_3 at 0 °C. After 1 h, 50 mL of ethyl acetate was added and the reaction mixture was washed successively with 1 N HCl, water, $NaHCO_3$, then dried and evaporated. The oily residue was treated with 2.2 equiv of BuLi at −78 °C for 1 h followed by addition of 0.6 equiv of diethyl chlorophosphate. The reaction mixture was warmed to 0 °C over 1 h and then quenched with saturated NH_4Cl. Column chromatography (silica gel, ethyl acetate) followed by hydrolysis using general method E gave **19** as a white powder (366 mg, 42% overall yield). Anal. ($C_{16}H_{18}K_2NO_6P \cdot KBr$) C, H, N. ^{1}H NMR (400 MHz, D_2O): δ 1.60−1.75 (m, 2H, CH_2); 2.50 (t, J = 7.6 Hz, 2H, $PhCH_2$); 2.87 (t, J = 7.2 Hz, 2H, CH_2N); 1.18 (d, J = 20 Hz, 2H, CH_2P); 6.70−7.30 (m, 9H, aromatic). ^{31}P NMR (D_2O): δ 4.4.

***N*-Hydroxy-*N*-[3-(4-methylbiphenyl)propyl]phosphonoacetamide (20).** Compound **20** was prepared in the same manner as **9**, using 4-methylphenylbenzaldehyde as starting material, as a white powder (175 mg, 48% overall yield). Anal. ($C_{18}H_{22}NO_5P \cdot 0.2HBr$) C, H, N. ^{1}H NMR (400 MHz, D_2O): δ 1.70−1.80 (m, 2H, CH_2); 2.21 (s, 3H, Me), 2.46 (t, J = 7.6 Hz, 2H, $PhCH_2$); 2.66 (d, J = 20 Hz, 2H, CH_2P); 3.42 (t, J = 7.2 Hz, 2H, CH_2N); 7.0−7.30 (m, 8H, aromatic). ^{31}P NMR (D_2O): δ 15.9.

***N*-[3-(3-Phenoxyphenyl)propyl]phosphonomalonamide Potassium Salt (21).** Amine **26** (1 mmol) was coupled with malonic acid monoethyl ester according to general method C to give the ethyl ester of **21**, which was then hydrolyzed with 3 equiv of KOH in $MeOH/H_2O$ for 1 h. The reaction mixture was acidified and extracted with ethyl acetate, and the organic layer was evaporated. The oily residue was dissolved in methanol, neutralized with KOH, and evaporated to give **21** as a white powder (250 mg mg, 66% overall yield). Anal. ($C_{18}H_{18}KNO_4 \cdot 0.25KCl \cdot 0.5H_2O$) C, H, N. ^{1}H NMR (400 MHz, D_2O): δ 1.80−1.90 (m, 2H, CH_2); 2.62 (t, J = 7.6 Hz, 2H, $PhCH_2$); 3.32 (s, 2H, CH_2COO); 3.33 (m, 2H, CH_2N); 6.70−7.40 (m, 9H, aromatic).

Enzyme and Biological Assays. CrtM Expression and Purification. CrtM with a histidine tag was overexpressed in *E. coli* BL21(DE3) cells and CrtM protein purified as described previously.[14] A 50 mL overnight culture was transferred into 1 L LB medium supplemented with 100 μg/mL ampicillin. Induction was carried out with 1 mM IPTG for 4 h at 37 °C, when the cell culture reached an OD of 0.6 at 600 nm. The cell extract was loaded onto a Ni-NTA column and CrtM eluted by using a 100 mL linear gradient of 0−0.5 M imidazole in 50 mM Tris-HCl buffer, pH 7.4.

CrtM Inhibition Assay. The condensation of farnesyl diphosphate was monitored by a continuous spectrophotometric assay for phosphate releasing enzymes.[1] The reaction buffer contained 50 mM Tris-HCl, 1 mM $MgCl_2$, 450 μM FPP, pH 7.4. The compounds investigated were preincubated with 2 μg of CrtM for 30 min at 20 °C. Reactions were carried out by using 96-well plates with 200 μL of reaction mixture in each well. The IC_{50} values were obtained by fitting the inhibition data to a normal dose−response curve in Origin 6.1 (OriginLab Corporation, Northampton, MA). The K_i values reported are calculated on the basis of the substrate concentrations used, the IC_{50} values found, and the kinetic constant for CrtM, as described previously.[14]

Staphyloxanthin Biosynthesis Inhibition Assay. The *S. aureus* strain used was the WT clinical isolate (Pig1). *S. aureus* was propagated in Todd-Hewitt broth (THB) or on THB agar (TBA; Difco, Detroit, MI). For in vitro pigment inhibition studies, *S. aureus* was cultured in THB (1 mL) in the presence of inhibitor compounds for 72 h, in duplicate. Prior to assay, the bacteria were centrifuged and washed twice in PBS. Staphyloxanthin was extracted with MeOH, and the OD was determined at 450 nm using a Perkin-Elmer MBA 2000 (Norwalk, CT) spectrophotometer. The IC_{50} values were obtained by fitting the OD data to a normal dose−response curve, using GraphPad PRISM.

Human SQS Enzyme Expression, Purification, and Inhibition Assay. *E. coli* expressing a human SQS construct were cultured in Luria−Bertani medium supplemented with kanamycin (30 μg/mL) and chloramphenicol (34 μg/mL) at 37 °C, until the cells reached an OD of 0.4 at 600 nm, and were then induced at 37 °C for 4 h by incubation with 1 mM isopropyl-1-thio-β-D-galactopyranoside. Cells were harvested by centrifugation (10 min, 4000 rpm) and resuspended in 10 mL of lysis/elution buffer (20 mM NaH_2PO_3, pH 7.4, 10 mM CHAPS, 2 mM $MgCl_2$, 10% glycerol, 10 mM mercaptoethanol, 500 mM NaCl, 10 mM imidazole, and a protease inhibitor cocktail), disrupted by sonication, and centrifuged at 16 000 rpm for 30 min. The supernatant (40 mL) was then applied to a HiTrap nickel-chelating HP column (Amersham Biosciences). Enzyme purification was performed according to the manufacturer's instructions using a Pharmacia FPLC system. Unbound protein was washed off with 50 mM imidazole, and then the His_6-HsSQS was eluted with 1 M imidazole. Purity was confirmed by SDS−PAGE electrophoresis. Fractions containing the enzyme were pooled and dialyzed against buffer A (25 mM sodium phosphate, pH 7.4, 20 mM NaCl, 2 mM dithiothreitol, 1 mM EDTA, 10% glycerol, 10% methanol), concentrated, then stored at −80 °C.

SQS activity was based on measuring the conversion of [^{3}H]FPP to [^{3}H]squalene. Final assay concentrations were 50 mM MOPS (pH 7.4), 20 mM $MgCl_2$, 5 mM CHAPS, 1% Tween-80, 10 mM DTT, 0.025 mg/mL BSA, 0.25 mM NADPH, and 7.5 ng of purified recombinant human SQS. The reaction was started with the addition of substrate (^{3}HFPP, 0.1 nmol, 2.22 × 10^6 dpm), and the final volume of the reaction was 200 μL. After incubation at 37 °C for 5 min, an amount of 40 μL of 10 M NaOH was added to stop the reaction, followed by 10 μL of a (100:1) mixture of 98% EtOH and squalene. The resulting mixtures were mixed vigorously by vortexing. Then 10 μL aliquots were applied to 2.5 cm × 10 cm channels of a silica gel thin layer chromatogram, and newly formed squalene was separated from unreacted substrate by chromatography in toluene−EtOAc (9:1). The region of the squalene band was scraped and immersed in Hydrofluor liquid scintillation fluid and assayed for radioactivity. IC_{50} values were calculated from the hyperbolic plot of percent of inhibition versus inhibitor concentration, using GraphPad PRISM.

Human Cell Growth Inhibition Assay. Three human cell lines MCF-7, NCI-H460, and SF-268 were obtained from the National Cancer Institute. Cells were cultured in RPMI-1640 medium supplemented with 10% fetal bovine serum and 2 mM L-glutamine at 37 °C in a 5% CO_2 atmosphere with 100% humidity. A broth microdilution method was used to calculate IC_{50} values for growth inhibition by each compound. Cells were inoculated at a density of 5000 cells/well into 96-well flat-bottom culture plates containing 10 μL of the test compound, previously half-log serial diluted (from 0.316 mM to 0.1 pM) for a final volume of 100 μL. Plates were then incubated for 4 days at 37 °C in a 5% CO_2 atmosphere at 100% humidity, after which an MTT ((3-(4,5-dimethylthiazole-2-yl)-2,5-diphenyltetrazolium bromide) cell proliferation assay (ATCC, Manassas, VA) was used to quantify cell viability. The IC_{50} values were obtained by fitting the OD data to a normal dose−response curve, using GraphPad PRISM.

Murine Model of Kidney Infection. The 10−12 week old CD1 male mice (Charles River Laboratory) were randomized into two groups at the start of the experiment and administered either 0.5 mg of BPH-652 or PBS control, ip, twice a day, starting on day 1 to day 2 (a total of eight doses). All mice were injected intraperitoneally (ip) with 10^8 early stationary phase *S. aureus* on day 0. After 3 days, animals were euthanized, kidneys homogenized in PBS, and plated on THA for quantitative bacterial culture.

Statistics. The significance of experimental differences in the mouse *in vivo* challenge studies were evaluated by use of the two-tailed Student's t test.

X-ray Crystallography. Native CrtM was eluted from Ni-NTA beads by incubation with factor Xa (Novagen) to cleave it from

the polyhistidine-containing N-terminal thioredoxin fusion tag. The cleaved product was equilibrated with buffer containing 150 mM NaCl, 5 mM DTT, 1 mM β-mercaptoethanol, 5% glycerol, and 20 mM Tris, pH 7.5 and then concentrated to 15 mg/mL. Native CrtM crystals (space group $P3_221$) were grown using the hanging-drop method by mixing equal amounts of reservoir with 0.12−0.58 M potassium sodium tartrate at room temperature. BPH-830 was incorporated by soaking crystals with a solution of **5** (10 mM in DMSO) for 3 h at room temperature. X-ray diffraction data were collected at SPXF beamline BL13B1 at the National Synchrotron Radiation Research Center (NSRRC), Hsinchu, Taiwan. All diffraction images were recorded using an ADSD Q210 CCD detector, and the data were indexed, integrated, and scaled by using the HKL2000 package.[21] The structure of the CrtM−**5** complex was determined by molecular replacement using CNS[22] using the refined native CrtM (PDB 2ZCO) as a search model. Iterative cycles of model building with Xtalview[23] and computational refinement with CNS were performed, in which 5% reflections were set aside for R_{free} calculation.[24] The stereochemical quality was assessed with the program PROCHECK.[25] Figures were obtained by using Pymol.[26]

Acknowledgment. This work was supported by the United States Public Health Service (Grant AI074832 to G.Y.L., Grant HD051796 to V.N., and Grants AI074233, GM073216, and GM65307 to E.O.). Y.S. was supported by a Leukemia and Lymphoma Society Special Fellowship. Diffraction data were obtained at the National Synchrotron Radiation Research Center of Taiwan and was supported by grants from Academia Sinica and the National Core Facility of High-Throughput Protein Crystallography (Grant SC95-3112-B-001-015-Y to A.H.-J.W.).

References

(1) Bancroft, E. A. Antimicrobial resistance: it's not just for hospitals. *JAMA, J. Am. Med. Assoc.* **2007**, *298* (15), 1803–1804.
(2) Klevens, R. M.; Morrison, M. A.; Nadle, J.; Petit, S.; Gershman, K.; Ray, S.; Harrison, L. H.; Lynfield, R.; Dumyati, G.; Townes, J. M.; Craig, A. S.; Zell, E. R.; Fosheim, G. E.; McDougal, L. K.; Carey, R. B.; Fridkin, S. K. Invasive methicillin-resistant *Staphylococcus aureus* infections in the United States. *JAMA, J. Am. Med. Assoc.* **2007**, *298* (15), 1763–1771.
(3) *Treating Infectious Diseases in a Microbial World: Report of Two Workshops on Novel Antibacterial Therapeutics*; National Research Council: Washington, DC, 2006; pp 21−22.
(4) Wang, R.; Braughton, K. R.; Kretschmer, D.; Bach, T. H.; Queck, S. Y.; Li, M.; Kennedy, A. D.; Dorward, D. W.; Klebanoff, S. J.; Peschel, A.; DeLeo, F. R.; Otto, M. Identification of novel cytolytic peptides as key virulence determinants for community-associated MRSA. *Nat. Med.* **2007**, *13* (12), 1510–1514.
(5) Escaich, S. Antivirulence as a new antibacterial approach for chemotherapy. *Curr. Opin. Chem. Biol.* **2008**, *12* (4), 400–408.
(6) Liu, G. Y.; Essex, A.; Buchanan, J. T.; Datta, V.; Hoffman, H. M.; Bastian, J. F.; Fierer, J.; Nizet, V. Staphylococcus aureus golden pigment impairs neutrophil killing and promotes virulence through its antioxidant activity. *J. Exp. Med.* **2005**, *202* (2), 209–215.
(7) Clauditz, A.; Resch, A.; Wieland, K. P.; Peschel, A.; Gotz, F. Staphyloxanthin plays a role in the fitness of *Staphylococcus aureus* and its ability to cope with oxidative stress. *Infect. Immun.* **2006**, *74* (8), 4950–4953.
(8) Pelz, A.; Wieland, K. P.; Putzbach, K.; Hentschel, P.; Albert, K.; Gotz, F. Structure and biosynthesis of staphyloxanthin from *Staphylococcus aureus*. *J. Biol. Chem.* **2005**, *280* (37), 32493–32498.
(9) Hammond, R. K.; White, D. C. Inhibition of vitamin K2 and carotenoid synthesis in Staphylococcus aureus by diphenylamine. *J. Bacteriol.* **1970**, *103* (3), 611–615.
(10) Hammond, R. K.; White, D. C. Inhibition of carotenoid hydroxylation in *Staphylococcus aureus* by mixed-function oxidase inhibitors. *J. Bacteriol.* **1970**, *103* (3), 607–610.
(11) Daum, R. S. Removing the golden coat of *Staphylococcus aureus*. *N. Engl. J. Med.* **2008**, *359* (1), 85–87.
(12) Walsh, C. T.; Fischbach, M. A. Inhibitors of sterol biosynthesis as *Staphylococcus aureus* antibiotics. *Angew. Chem., Int. Ed. Engl.* **2008**, *47* (31), 5700–5702.
(13) Haebich, D.; von Nussbaum, F. "Superbugs bunny" outsmarts our immune defense. *ChemMedChem* **2008**, *3* (8), 1173–1177.
(14) Liu, C. I.; Liu, G. Y.; Song, Y.; Yin, F.; Hensler, M. E.; Jeng, W. Y.; Nizet, V.; Wang, A. H.; Oldfield, E. A cholesterol biosynthesis inhibitor blocks *Staphylococcus aureus* virulence. *Science* **2008**, *319* (5868), 1391–1394.
(15) Magnin, D. R.; Biller, S. A.; Dickson, J. K., Jr.; Logan, J. V.; Lawrence, R. M.; Chen, Y.; Sulsky, R. B.; Ciosek, C. P., Jr.; Harrity, T. W.; Jolibois, K. G.; et al. 1,1-Bisphosphonate squalene synthase inhibitors: interplay between the isoprenoid subunit and the diphosphate surrogate. *J. Med. Chem.* **1995**, *38* (14), 2596–2605.
(16) Magnin, D. R.; Biller, S. A.; Chen, Y.; Dickson, J. K., Jr.; Fryszman, O. M.; Lawrence, R. M.; Logan, J. V.; Sieber-McMaster, E. S.; Sulsky, R. B.; Traeger, S. C.; Hsieh, D. C.; Lan, S. J.; Rinehart, J. K.; Harrity, T. W.; Jolibois, K. G.; Kunselman, L. K.; Rich, L. C.; Slusarchyk, D. A.; Ciosek, C. P., Jr. α-Phosphonosulfonic acids: potent and selective inhibitors of squalene synthase. *J. Med. Chem.* **1996**, *39* (3), 657–660.
(17) Rieger, C. E.; Lee, J.; Turnbull, J. L. A continuous spectrophotometric assay for aspartate transcarbamylase and ATPases. *Anal. Biochem.* **1997**, *246* (1), 86–95.
(18) Song, Y.; Lin, F.-Y.; Yin, F.; Hensler, M.; Poveda, C. A. R.; Mukkamala, D.; Cao, R.; Wang, H.; Morita, C. T.; Pacanowska, D. G.; Nizet, V.; Oldfield, E. Phosphonosulfonate are potent, selective inhibitors of dehydrosqualene synthase and staphyloxanthin biosynthesis in *Staphylococcus aureus*. *J. Med. Chem.* **2009**, *52* (4), 976–988.
(19) Mukkamala, D.; No, J. H.; Cass, L. M.; Chang, T. K.; Oldfield, E. Bisphosphonate inhibition of a Plasmodium farnesyl diphosphate synthase and a general method for predicting cell-based activity from enzyme data. *J. Med. Chem.* **2008**, *51* (24), 7827–7833.
(20) *Molecular Operating Environment (MOE)*; Chemical Computing Group, Inc.: Montreal, Quebec, 2006.
(21) Otwinowski, Z.; Minor, W. ; Processing of X-ray diffraction data collected in oscillation mode. *Macromol. Crystallogr.* **1997**, *276*, 307–326.
(22) Brunger, A. T.; Adams, P. D.; Clore, G. M.; DeLano, W. L.; Gros, P.; Grosse-Kunstleve, R. W.; Jiang, J. S.; Kuszewski, J.; Nilges, M.; Pannu, N. S.; Read, R. J.; Rice, L. M.; Simonson, T.; Warren, G. L. Crystallography & NMR system: a new software suite for macromolecular structure determination. *Acta Crystallogr., Sect. D: Biol. Crystallogr.* **1998**, *54* (Part 5), 905–921.
(23) McRee, D. E. XtalView Xfit. A versatile program for manipulating atomic coordinates and electron density. *J. Struct. Biol.* **1999**, *125* (2V3), 156–165.
(24) Brunger, A. T. Assessment of phase accuracy by cross validation: the free *R* value. Methods and applications. *Acta Crystallogr. D* **1993**, *49* (1), 24–36.
(25) Laskowski, R. A.; MacArthur, M. W.; Moss, D. S.; Thornton, J. M. PROCHECK: a program to check the stereochemical quality of protein structures. *J. Appl. Crystallogr.* **1993**, *26*, 283–291.
(26) DeLano, W. L. *The PyMOL Molecular Graphics System*; DeLano Scientific: Palo Alto, CA, 2008; http://www.pymol.org.
(27) Wallace, A. C.; Laskowski, R. A.; Thornton, J. M. Ligplot: a program to generate schematic diagrams of protein−ligand interactions. *Protein Eng.* **1995**, *8*, 127–134.

JM9001764